

Partitions of a Simplex Leading to Accurate Spectral (Finite) Volume Reconstruction

Qian-Yong Chen*

Abstract

In this paper, we present several systematic techniques, based on the Voronoi diagram and its variants, to partition a one and two-dimensional simplex. The Fekete points are used as input to generate the Voronoi diagram, as they concentrate near the edges and are almost optimal for polynomial interpolation in a simplex.

Spectral (finite) volume reconstructions on the resulted partitions have small Lebesgue constants. When using the Dubiner basis, the reconstruction matrix is well conditioned. Moreover, the total number of edges of the partitions (the total work when being used in spectral volume methods) is shown to be at most twice the minimum number of edges of all partitions for reconstructions of the same order accuracy. These suggest that the obtained partitions are well suited for spectral volume methods and other numerical methods which rely on reconstructions from cell averages.

*Division of Applied Mathematics, Brown University, Box F, Providence, RI 02912 (cqy@dam.brown.edu).

1 Introduction

In [10], Wang proposed a new finite volume (FV) method, named spectral volume (SV) method, for hyperbolic conservation laws. The spectral volume method has several good properties: high-order accurate, conservative, geometrically flexible, and computationally efficient. (A comparison with the discontinuous Galerkin methods is given in [12].) In the spectral volume method, a volume or a cell (named spectral volume) is partitioned into non-overlapping sub-cells named control volumes (CVs). Then cell-averaged solutions on the control volumes are used to perform high order reconstructions, i.e., spectral volume reconstructions. The spectral volume reconstruction is different from the reconstruction procedure of previous finite volume methods, which employs cell-averaged solutions on neighbour cells to perform the reconstruction.

The spectral volume reconstruction is basically an approximation problem. Given a smooth function and an approximation space, the accuracy of the spectral volume reconstructions only depends on the partition of the spectral volume. Not all partitions produce good results. For example, uniform partitions [11] yield bad results for high-order reconstructions because of the Runge phenomenon. As far as we know, no systematic technique has been developed to partition an m -dimensional simplex, $S^m \subset R^m$, except that in [11] Wang gave a few partitions for up to the fourth-order reconstruction on a standard equilateral triangle. It is difficult to directly build good high order partitions because there are too many parameters such as the position of points, the number of edges for each subcell and the topology of the subcells. Of course, one can compute the so called L^2 optimal partitions as [1]. But even for one-dimensional case, the L^2 optimal partitions are not as satisfactory as the correspondents for the interpolation [9].

However, another approximation problem on a simplex, the interpolation based on node values, has been extensively studied in the past (see [6] and the references therein). Some almost optimal nodal sets for polynomial interpolation on a two-dimensional simplex are given in [1], [6] and [8]. In this paper, we develop several systematic techniques, based on the well-known Voronoi diagram and its variants with those optimal nodal sets as the input, to generate partitions of a one and two-dimensional simplex. Using these techniques, we obtained partitions for up to the 14-th

order polynomial reconstruction on an equilateral triangle.

The remaining of the paper is organized as follows. In Sec. 2, we restate the spectral volume reconstruction problem on a two-dimensional simplex. The Lebesgue constant is introduced as one measurement of the quality of spectral volume reconstructions. Section 3 describes the systematic techniques to partition a one and two-dimensional simplex. Finally, we summarize the paper and make some concluding remarks in Sec. 4.

2 Spectral Volume Reconstruction

In this section, we define the spectral volume reconstruction problem on an equilateral triangle, S^2 . Some issues related to the quality of spectral volume reconstructions are also addressed.

The spectral volume reconstruction is a key element of the recently proposed spectral volume method [10, 11], in which a target cell is divided into non-overlapping sub-cells. The cell-averaged solutions on the sub-cells are then used to reconstruct an approximate solution on the target cell. The number of sub-cells is the same as the dimension of the approximation space. In general, the approximation space can consist of any functions. Here, we focus on the space of polynomials of degree up to n , denoted as P_2^n . The dimension of this approximation space is

$$N_n^2 = \dim P_2^n = \binom{2+n}{2}. \quad (1)$$

$N = N_n^2$ and $P^n = P_2^n$ will be used to simplify the notations if there is no confusion.

Then the spectral volume reconstruction problem can be formally stated as follows.

SV Reconstruction Problem on S^2 : *Given any continuous function $u(x, y)$ on S^2 , i.e., $u \in C^0(S^2)$, the spectral volume reconstruction is to*

1. *Construct a partition Π_n of S^2 :*

$$S^2 = C_1 \cup \dots \cup C_N,$$

where $\{C_1, \dots, C_N\}$ are N non-overlapping sub-cells;

2. *Compute the projection $I_{\Pi_n} u \in P^n$ such that*

$$\int_{C_i} (I_{\Pi_n} u) dV = \int_{C_i} u(x, y) dV, \quad i = 1, \dots, N, \quad (2)$$

i.e., u and $I_{\Pi_n} u$ have the same average on all the sub-cells.

The projection, $I_{\Pi_n} u$, can be computed once the partition Π_n is known. Express $I_{\Pi_n} u$ as a series sum of a complete basis of P^n , $\{p_1(x, y), \dots, p_N(x, y)\}$,

$$I_{\Pi_n} u = \sum_{i=1}^N a_i p_i(x, y). \quad (3)$$

Denote \bar{u}_i as the average of $u(x, y)$ over the sub-cell C_i , i.e.,

$$\bar{u}_i = \frac{1}{V_i} \int_{C_i} u(x, y) dV, \quad i = 1, \dots, N, \quad (4)$$

where V_i is the area of C_i . Plug (3) and (4) into (2), and rewrite the new equation into a matrix form

$$A a = \bar{u}, \quad (5)$$

where $\bar{u} = (\bar{u}_1, \dots, \bar{u}_N)^T$, $a = (a_1, \dots, a_N)^T$, and the reconstruction matrix A takes the form

$$A = \begin{pmatrix} \frac{1}{V_1} \int_{C_1} p_1(x, y) dV & \cdots & \frac{1}{V_1} \int_{C_1} p_N(x, y) dV \\ \cdots & \cdots & \cdots \\ \frac{1}{V_N} \int_{C_N} p_1(x, y) dV & \cdots & \frac{1}{V_N} \int_{C_N} p_N(x, y) dV \end{pmatrix}. \quad (6)$$

When the partition is non-singular, i.e., the matrix A is non-singular, we solve Eq. (5) and substitute the solution a back into the expression (3) to obtain

$$I_{\Pi_n} u = \sum_{i=1}^N \bar{u}_i L_i(x, y), \quad (7)$$

where the cardinal basis functions $L = (L_1(x, y), \dots, L_N(x, y))$ are given as

$$L = (p_1(x, y), \dots, p_N(x, y)) A^{-1}. \quad (8)$$

Then we equip the space P^n and $C^0(S^2)$ with an L^∞ norm (supremum-norm, denoted as $\|\cdot\|$) and the induced functional norm

$$\|I_{\Pi_n}\| = \sup_{\|u\| \neq 0} \frac{\|I_{\Pi_n} u\|}{\|u\|}.$$

Since $|\bar{u}_i| \leq \|u\|$ for $i = 1, \dots, N$, one can show that

$$\|I_{\Pi_n}\| = \max_{(x,y) \in S^2} \sum_{i=1}^N |L_i(x, y)|. \quad (9)$$

2.1 Error of Spectral Volume Reconstruction

One measurement of the quality of spectral volume reconstruction is the error. Similar to that of polynomial interpolation, the error of spectral volume reconstruction is bounded from below as

$$\|u - u^*\| \leq \|u - I_{\Pi_n} u\|, \quad (10)$$

where u^* is the optimal approximating polynomial whose existence is guaranteed by the continuity of $u(x, y)$ [2]. Although it is difficult to determine such optimal approximation for general functions, it enables us to evaluate the quality of other approximations. From the linearity of the projection operator I_{Π_n} and the fact that $I_{\Pi_n} f = f, \forall f \in P^n(S^2)$, one can verify that

$$\|u - I_{\Pi_n} u\| \leq (1 + \Lambda(\Pi_n)) \|u - u^*\|, \quad (11)$$

where

$$\Lambda(\Pi_n) = \|I_{\Pi_n}\| = \max_{(x,y) \in S^2} \sum_{i=1}^N |L_i(x, y)| \quad (12)$$

is called the Lebesgue constant of the operator I_{Π_n} .

From the way to compute $I_{\Pi_n} u$ as previously described, one can show that the Lebesgue constant only depends on the partition Π_n when the approximation space is fixed.

Lemma 1 *When the approximation space is fixed, the partition determines the Lebesgue constant.*

Proof: From the definition of the Lebesgue constant (c.f. (12)), it is enough to show that the same cardinal basis functions will be obtained for two different basis sets of the approximation space.

Choose another basis set, $(q_1(x, y), \dots, q_N(x, y)) = (p_1(x, y), \dots, p_N(x, y)) \cdot T$, where T is a constant non-singular matrix. According to Eq. (6), the new reconstruction matrix is

$$\tilde{A} = A \cdot T.$$

So the new cardinal basis is

$$\tilde{L} = (q_1, \dots, q_N) \cdot \left(\tilde{A}\right)^{-1} = (p_1, \dots, p_N) \cdot T \cdot T^{-1} A^{-1} = L,$$

which proves the lemma. ■

According to (11) and (10), the magnitude of the Lebesgue constant reflects how close the spectral volume reconstruction is to the optimal polynomial approximation. Therefore, spectral volume reconstructions with small Lebesgue constant are preferred. For simplicity, we only consider partitions with sub-cells being convex polygons with straight edges. However, this might

keep us from obtaining spectral volume reconstructions with Lebesgue constant as small as those of polynomial interpolation in [8] and [6].

Another important issue is the work load when the spectral volume reconstruction procedure is used in solving partial differential equations. As shown in [11, 10], the work load is roughly proportional to the total number of edges of the partition. Hence the optimal partition should have minimum number of edges and lead to the smallest Lebesgue constant. If one wants to optimize the partition, one needs to minimize both the number of edges and the Lebesgue constant at the same time, which apparently is not an easy task. We made no such effort in this paper.

We also want to emphasize that it is necessary that the reconstruction matrix A is well-conditioned for high-order spectral volume reconstructions because of the finite precision of computers. For polynomial interpolation on a triangle, this is usually achieved by choosing the Dubiner basis [4] instead of the notorious monomials, provided the nodal set is good.

3 Partitions from Voronoi Diagram and Its Variants

In this section, we describe a few systematic techniques to partition a one and two-dimensional simplex by using the Voronoi diagram and its variants.

3.1 The Voronoi Diagram and Its Variants

The following definition is a generalization of the two-dimensional Voronoi diagram [7, 3].

Definition 1 (*Voronoi Diagram*) Given N distinct input points $S = \{p_1, \dots, p_N\}$ in R^m , the Voronoi diagram is a partition of R^m into N non-overlapping polyhedral regions: $\{V_1, \dots, V_N\}$, such that $p_i \in V_i$, $i = 1, \dots, N$, and the Voronoi cell V_i is the set of points in R^m which are closer to p_i than to any other points in S , i.e.,

$$V_i = \{x \in R^m : |x - p_i| \leq |x - q|, \forall q \in S - p_i\}, \quad (13)$$

where $|x - y|$ represents the Euclidean distance between x and y (other distance functions can also be used).

All Voronoi cells and faces form a cell complex whose vertices and edges are called *Voronoi vertices* and *Voronoi edges*. The unbounded edges are also called *Voronoi rays*. When the input points, $\{p_1, \dots, p_N\}$, are in the plane ($m=2$), we can bound the number of the Voronoi vertices and Voronoi edges by the following theorem [7, 3].

Theorem 1 For $N \geq 3$, in the Voronoi diagram of N distinct points on the plane, the number of Voronoi vertices is at most $2N - 5$; the number of Voronoi edges is at most $3N - 6$.

When the input points are on a triangle, it is straightforward to generate a partition of the triangle from the Voronoi diagram, e.g., Fig. 1. So we can partition a triangle by choosing the input points and computing the Voronoi diagram. Furthermore, each Voronoi vertex (the circles in Fig. 1) is the circumcenter of one triangle with vertices being three input points. One can get a few variants of the Voronoi diagram, and thus different partitions, by replacing each Voronoi vertex

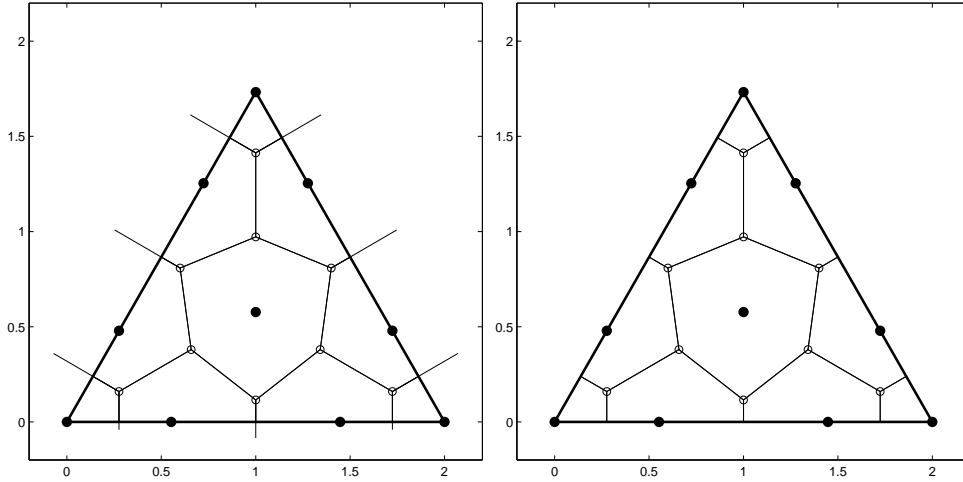


Figure 1: Partition of a triangle from the Voronoi diagram of given points on the triangle. On the left graph, the dark dots are the input points; the circles are the Voronoi vertices; the thin solid lines are the Voronoi edges. The right graph displays the partition.

(circumcenter) with the corresponding incenter, centroid or any other point related to that triangle. We recall that for a triangle, the circumcenter is the center of its circumcircle, the incenter is the center of its incircle, and the centroid is the intersection of the triangle's three triangle medians.

3.2 Partitions of S^1

S^1 is simply a line segment. Without loss of generality, let $S^1 = [-1, 1]$. One can generate a partition from any given input points set as follows. Suppose $-1 = x_0 < x_1 < \dots < x_n = 1$ are the input points. Take $y_0 = x_0, y_{n+1} = x_n$ and $y_i = (x_i + x_{i-1})/2, i = 1, \dots, n$. The points $\{y_i\}$ then define a partition: $V_i = [y_i, y_{i+1}], i = 0, \dots, n$. A different points set will yield a different partition. Table 1 includes the Lebesgue constants corresponding to the Legendre Gauss-Lobatto (LGL) and Chebyshev Gauss-Lobatto (CGL) quadrature points. Note that the Legendre Gauss-Lobatto points are actually the Fekete points in the interval [5]. Λ^{LGL} and Λ^{CGL} represent the Lebesgue constants of polynomial interpolation with the Legendre Gauss-Lobatto and Chebyshev Gauss-Lobatto points. $\Lambda_{\mathbf{V}}^{\text{LGL}}$ and $\Lambda_{\mathbf{V}}^{\text{CGL}}$ represent the Lebesgue constants for the spectral volume reconstruction on the partitions with LGL and CGL points being the input. $\Lambda_{\mathbf{V}}^{\text{Eq}}$ denotes the Lebesgue constant for spectral volume reconstruction on the uniform mesh, i.e., all sub-cells have the same size.

Note that the Lebesgue constants of spectral volume reconstruction on the partitions from both LGL and CGL points are less than twice those of polynomial interpolation, which are very close to the Lebesgue constants of the optimal nodal set [6]. In summary,

$$\Lambda_V^{\text{Eq}} > \Lambda_V^{\text{LGL}} > \Lambda_V^{\text{CGL}} > \Lambda^{\text{CGL}} > \Lambda^{\text{LGL}}. \quad (14)$$

Table 1: Lebesgue constants for one-dimensional spectral volume reconstruction and interpolation. n : the order of spectral volume reconstruction or interpolation.

n	Λ^{LGL}	Λ_V^{LGL}	Λ^{CGL}	Λ_V^{CGL}	Λ_V^{Eq}
2	1.2500	2.6667	1.2500	2.6667	3.3333
3	1.5000	3.0299	1.6667	2.8095	5.3333
4	1.6359	3.2702	1.7987	2.8607	8.5333
5	1.7786	3.4451	1.9889	2.8846	13.8666
6	1.8737	3.5800	2.0825	2.8976	23.0095
7	1.9724	3.6881	2.2022	2.9054	39.0095
8	2.0456	3.7773	2.2747	2.9106	67.4539
9	2.1210	3.8526	2.3619	2.9141	118.6539
10	2.1805	3.9172	2.4210	2.9439	211.7448
11	2.2415	3.9735	2.4894	3.0627	382.4115
12	2.2917	4.0230	2.5393	3.1503	697.4884
13	2.3428	4.0671	2.5957	3.2478	1282.6313
14	2.3862	4.1067	2.6388	3.3229	2374.8979
15	2.4303	4.1424	2.6867	3.4054	4422.8979
16	2.4684	4.1749	2.7247	3.4709	8227.9568
17	2.5072	4.2047	2.7664	3.5422	15559.7345
18	2.5412	4.2320	2.8003	3.6004	29356.7872
19	2.5758	4.2573	2.8371	3.6631	55571.1872
20	2.6066	4.2807	2.8678	3.7154	105503.3776

3.3 Partitions of S^2

We only study the standard equilateral triangle S^2 (c.f. Fig. 1) because any other triangle can be obtained from a linear transformation of this triangle. The linear transformation will not change the Lebesgue constant of spectral volume reconstruction, which will be shown as below.

Lemma 2 *Suppose the standard equilateral triangle S^2 has a partition $\Pi_n = \{C_1, \dots, C_N\}$. Let \tilde{S} be a triangle defined on $\xi - \eta$ plane, which can be obtained from a non-singular linear*

transformation of S^2 . If the partition of \tilde{S} , $\tilde{\Pi}_n = \{\tilde{C}_1, \dots, \tilde{C}_N\}$, is obtained from Π_n by the same linear transformation, then the spectral volume reconstructions on \tilde{S} and S^2 have the same Lebesgue constant.

Proof: Denote \tilde{V}_i as the area of sub-cell \tilde{C}_i . Use \tilde{A} and \tilde{L} to represent the reconstruction matrix and cardinal basis set on \tilde{S} . For S^2 , the same notations will be used as those in Sec.2.

From the definition of the Lebesgue constant, it suffices to show that

$$\tilde{L}(\xi, \eta) = L(x, y), \quad \forall (\xi, \eta) \in \tilde{S} \text{ or } (x, y) \in S^2.$$

According to (8),

$$\begin{cases} L(x, y) = (p_1(x, y), \dots, p_N(x, y)) A^{-1} \\ \tilde{L}(\xi, \eta) = (p_1(\xi, \eta), \dots, p_N(\xi, \eta)) \tilde{A}^{-1} \end{cases}.$$

Since the transformation, $(\xi, \eta) \leftarrow (x, y)$, is linear, there exists a constant matrix T such that

$$(p_1(\xi, \eta), \dots, p_N(\xi, \eta)) = (p_1(x, y), \dots, p_N(x, y)) \cdot T. \quad (15)$$

T is also non-singular as the transformation is non-singular. (The non-singularity of T can be proved by evaluating Eq. (15) at N distinct points.) Plug Eq. (15) into the reconstruction matrix

$$\tilde{A} = \begin{pmatrix} \frac{1}{\tilde{V}_1} \int_{\tilde{C}_1} \tilde{p}_1(\xi, \eta) d\tilde{V} & \dots & \frac{1}{\tilde{V}_1} \int_{\tilde{C}_1} \tilde{p}_N(\xi, \eta) d\tilde{V} \\ \dots & \dots & \dots \\ \frac{1}{\tilde{V}_N} \int_{\tilde{C}_N} \tilde{p}_1(\xi, \eta) d\tilde{V} & \dots & \frac{1}{\tilde{V}_N} \int_{\tilde{C}_N} \tilde{p}_N(\xi, \eta) d\tilde{V} \end{pmatrix}$$

to obtain

$$\tilde{A} = A \cdot T.$$

Hence,

$$\tilde{L}(\xi, \eta) = (p_1(\xi, \eta), \dots, p_N(\xi, \eta)) \tilde{A}^{-1} = (p_1(x, y), \dots, p_N(x, y)) \cdot T \cdot (A \cdot T)^{-1} = L(x, y). \quad \blacksquare$$

The first kind of partitions, denoted as $\Pi_{\text{out}}^{\mathbf{F}}$, are from the Voronoi diagram¹ of the two-dimensional Fekete points [8] on the triangle. As previously mentioned, each Voronoi vertex is

¹Fortune's code is used to compute the 2-D Voronoi Diagram

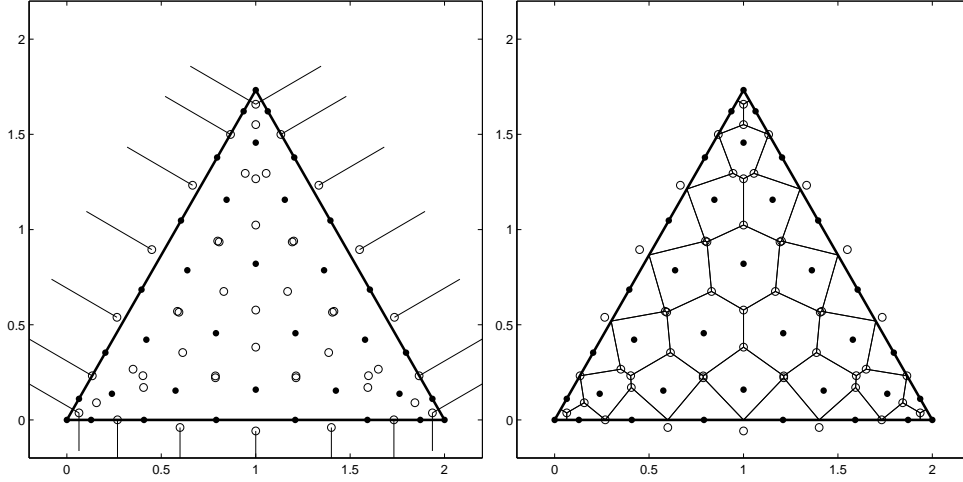


Figure 2: The 7-th order partition from the Voronoi diagram of given Fekete points. On the left graph, the thin solid lines are the Voronoi rays; the circles are the Voronoi vertices. The right graph is the partition. The outside Voronoi vertices are also plotted for clarity.

the circumcenter of one triangle with vertices being three input points. So there might be some Voronoi vertices which are outside the big equilateral triangle. When this happens, the partition is not as obvious as shown in Fig. 1. But as demonstrated in Fig. 2, we can obtain a partition by replacing each outside Voronoi vertex with the intersection point of the corresponding Voronoi ray and the edge of the big equilateral triangle. With this strategy, we generate partitions up to the 14-th order (Fig. 3). The Lebesgue constants of spectral volume reconstruction are listed in Tab. 2. The number of distinct edges is bounded as follows.

Theorem 2 *The total number of edges in the partition, Π_{out}^F is less than twice the minimum number of edges of any partition leading to the same order spectral volume reconstruction.*

Proof: For the n -th order partition Π_{out}^F , according to Theorem 1, the Voronoi diagram contributes at most $(3N - 6)$ to the total number of edges, where $N = \binom{2+n}{2}$ (c.f. Eq. (1)) is the total number of input points on the triangle. Besides that, there are $3(n + 1)$ edges which lie on the edges of the big equilateral triangle. So the total number of edges of the n -th partition Π_{out}^F is at most

$$3N - 6 + 3(n + 1) = \frac{3}{2}(n^2 + 5n). \quad (16)$$

Consider an arbitrary partition leading to an n -th order spectral volume reconstruction. Denote X as the number of edges of the partition which are on the edges of the big equilateral triangle, and

Y as the number of remaining edges (called *inside edges* since they are inside the big equilateral triangle). Clearly, $X = 3(n + 1)$. Since an n -th order reconstruction needs N polygons, each of which has at least three edges, one can show that

$$X + 2Y \geq 3N,$$

where the coefficient before Y is due to the fact that each inside edge belongs to two polygons. Thus, the minimum number of distinct edges for any n -th order partition satisfies

$$X + Y \geq X + \frac{3N - X}{2} = 3(n + 1) + \frac{3N - 3(n + 1)}{2} = \frac{3}{4}(n^2 + 5n + 4).$$

Comparing the above equation with (16) proves the theorem. ■

However, this simple usage of the Voronoi diagram does not yield very small Lebesgue constants, as shown in Fig 7, for high order spectral volume reconstructions.

We derive the second kind of partitions (denoted as $\Pi_{\mathbf{in}}^{\mathbf{F}}$) from one variant of the Voronoi diagram in which each Voronoi vertex is replaced by the corresponding incenter. By doing that, the structure of the partitions is more similar to the structure of the input points in the sense of layered structures and concentration near the edges (see Fig. 3 and 4). This is due to the fact that the incenter of a triangle is always inside the triangle. We believe that the layered structure and being concentrated near the edges of the sub-cells are crucial for the partition to produce small Lebesgue constants. As expected, the partition $\Pi_{\mathbf{in}}^{\mathbf{F}}$ produces smaller Lebesgue constants than $\Pi_{\mathbf{out}}^{\mathbf{F}}$ for most cases of the spectral volume reconstructions of order up to 14 (Tab. 2).

Unfortunately, as shown in Fig. 7, there is a sudden increase in the Lebesgue constants of the 8-th or higher order $\Pi_{\mathbf{in}}^{\mathbf{F}}$ partitions. By examining Fig. 4 more carefully, we notice that the layered structure is a bit “distorted” in the place close to the edges of the big triangle. The “distortion” is responsible for the sudden increase of the Lebesgue constants.

The Fekete points set itself has a very nice structure (Fig. 5), based on which we come up with the third kind of partitions, denoted as $\Pi_{\mathbf{mass}}^{\mathbf{F}}$. There are three steps to build the partition, which are demonstrated in Fig. 5. At first, we concatenate the input points layer by layer (see the left graph of Fig. 5). Then we construct a triangular mesh as shown in the middle graph of Fig.

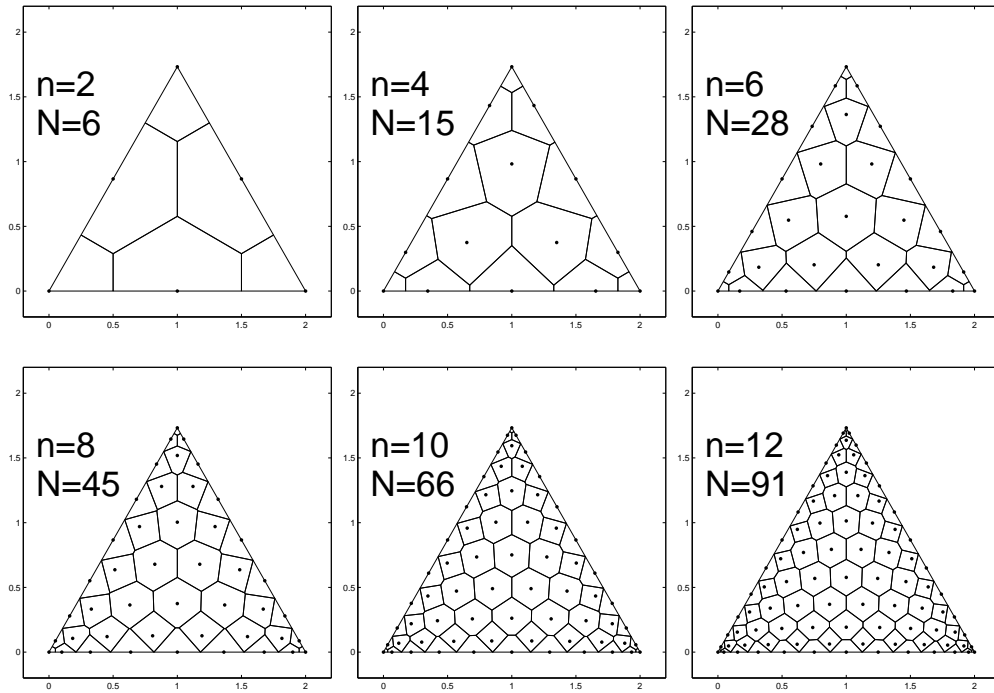


Figure 3: Partition Π_{out}^F . n : Order of SV reconstruction; N : Number of sub-cells; $'\cdot'$: input Fekete points on the triangle.

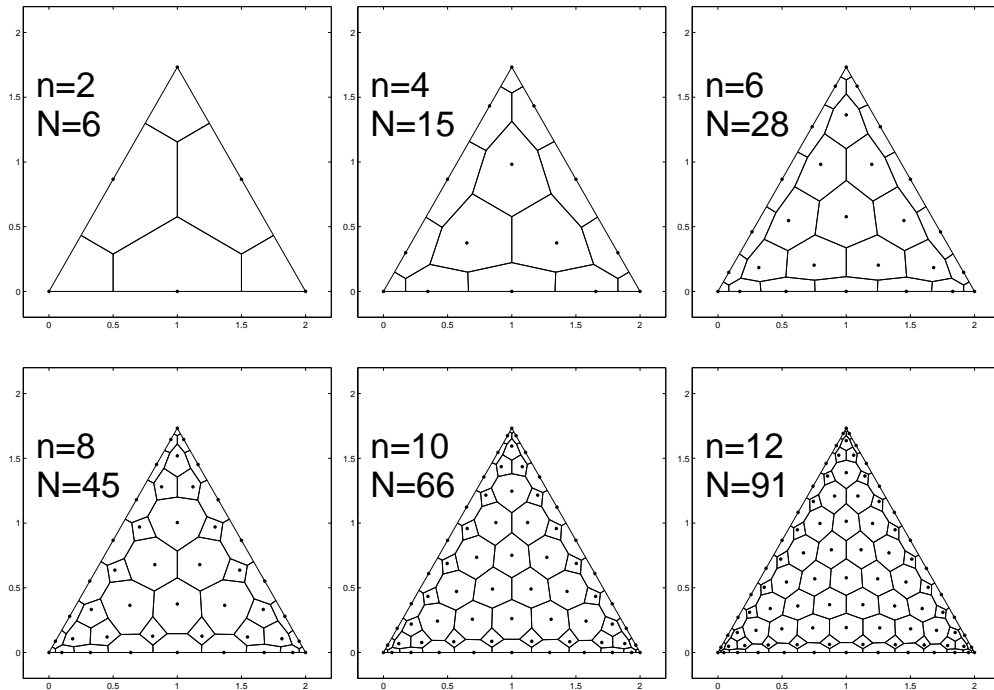


Figure 4: Partition Π_{in}^F . n : Order of SV reconstruction; N : Number of sub-cells; $'\cdot'$: input Fekete points on the triangle.

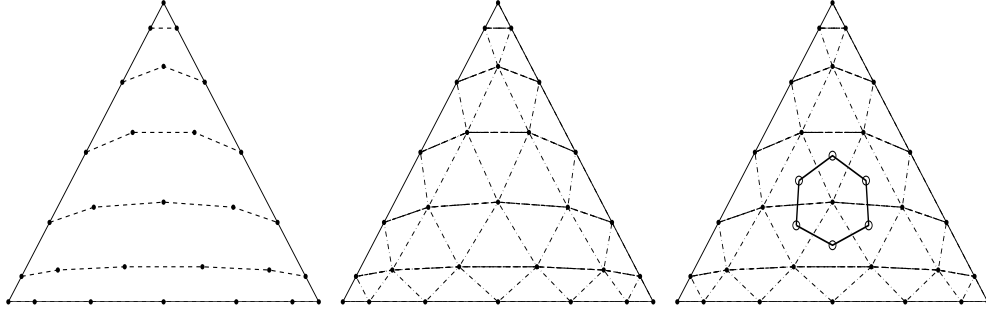


Figure 5: Three steps to construct the partition Π_{out}^F . '•': input Fekete points. Left: the layered structure of Fekete points; Middle: the triangular mesh; Right: the method to build the polygon (thick line) for one input point. 'o': vertices of the polygon.

5. Finally, for each input point inside the big triangle, we construct a polygon by connecting the centroid (or any other point) of the small triangles those share the input point (see the right graph of Fig. 5). When an input point is on the edge of the big triangle, one can construct a polygon containing it by using two more points on the edges of the big equilateral triangle. Some examples of the partitions are displayed in Fig. 6. We also tried to use the incenter instead of centroid of those small triangles. It leads to almost the same Lebesgue constants as the centroid does.

The same upper bound holds for the number of edges of the partitions Π_{in}^F and Π_{mass}^F .

Theorem 3 *The total number of edges in the partition Π_{in}^F or Π_{mass}^F , is less than twice the minimum number of edges for any partition leading to the same order SV reconstruction.*

The proof is omitted as it is basically the same as that of **Theorem 2**.

For comparison, we also compute the Lebesgue constants of the partition $\Pi_{\mathbf{V}}^{\text{Eq}}$, which is from the Voronoi diagram of equispaced (in the area coordinate system) points on the equilateral triangle. The Lebesgue constants for all partitions are listed in Tab. 2. And Table 3 contains the 2-norm condition numbers of the reconstruction matrix when the Dubiner basis is used. Figure 7 displays the ratios of the Lebesgue constants from the above partitions to those of the polynomial interpolations based on the Fekete points.

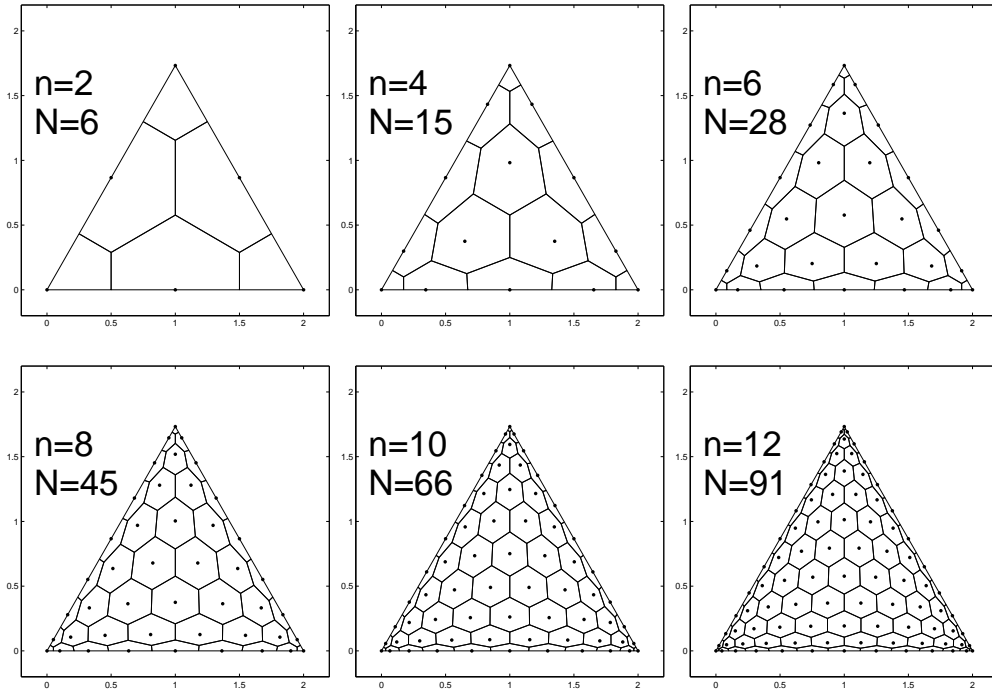


Figure 6: Partition Π_{mass}^F . n : Order of SV reconstruction; N : Number of sub-cells; '·': input Fekete points on the triangle.

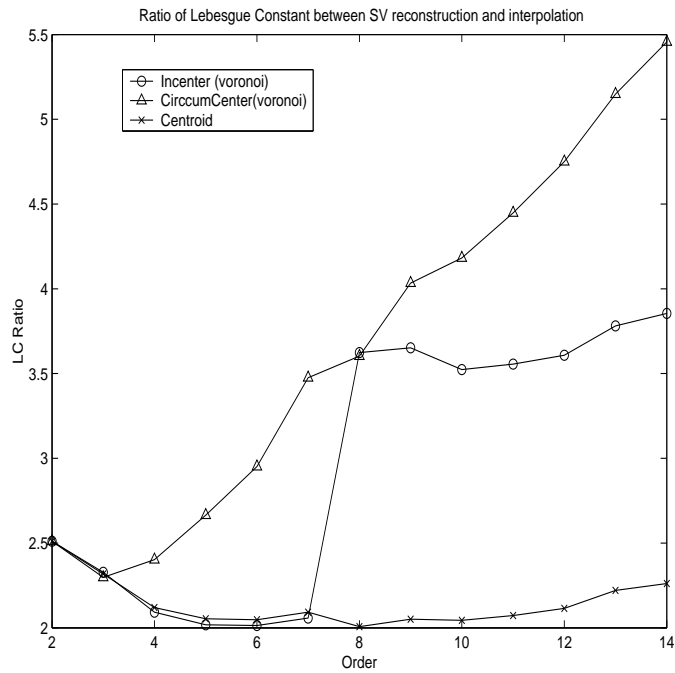


Figure 7: The ratio of the Lebesgue constants of two-dimensional spectral volume reconstructions to those of the interpolation on Fekete points. '△': Π_{out}^F partition; '○': Π_{in}^F partition; '×': Π_{mass}^F partition;

Table 2: Lebesgue constants for two-dimensional spectral volume reconstruction and interpolation. $\Lambda^{\mathbf{F}}$ stands for the Lebesgue constant for the interpolations with Fekete points. $\Lambda_{\text{out}}^{\mathbf{F}}$, $\Lambda_{\text{in}}^{\mathbf{F}}$, $\Lambda_{\text{mass}}^{\mathbf{F}}$, and $\Lambda_{\mathbf{V}}^{\text{Eq}}$ represent the Lebesgue constants for the SV reconstruction on the partition $\Pi_{\text{out}}^{\mathbf{F}}$, $\Pi_{\text{in}}^{\mathbf{F}}$, $\Pi_{\text{mass}}^{\mathbf{F}}$ and $\Pi_{\mathbf{V}}^{\text{Eq}}$ respectively.

n	N_n	$\Lambda^{\mathbf{F}}$	$\Lambda_{\text{out}}^{\mathbf{F}}$	$\Lambda_{\text{in}}^{\mathbf{F}}$	$\Lambda_{\text{mass}}^{\mathbf{F}}$	$\Lambda_{\mathbf{V}}^{\text{Eq}}$
2	6	1.6600	4.1673	4.1673	4.1673	4.167
3	10	2.1053	4.8374	4.8999	4.8797	6.031
4	15	2.7227	6.5407	5.6978	5.7719	8.768
5	21	3.5950	9.5786	7.2547	7.3822	12.911
6	28	4.1706	12.3091	8.3994	8.5399	19.384
7	36	4.9271	17.1220	10.1359	10.3084	29.774
8	45	5.8785	21.1783	21.3010	11.8001	46.859
9	55	6.8006	27.4297	24.8328	13.9493	75.523
10	66	7.9620	33.2994	28.0529	16.2751	124.448
11	78	9.4765	42.1511	33.6964	19.6389	209.165
12	91	11.0552	52.5173	39.8890	23.3799	357.725
13	105	13.2040	67.9809	49.9275	29.3272	620.707
14	120	15.9693	87.1305	61.5641	36.1131	1090.979

Table 3: The 2-norm condition numbers of the spectral volume reconstruction matrix on the two-dimensional partitions.

n	N_n	$\Pi_{\text{out}}^{\mathbf{F}}$	$\Pi_{\text{in}}^{\mathbf{F}}$	$\Pi_{\text{mass}}^{\mathbf{F}}$	$\Pi_{\mathbf{V}}^{\text{Eq}}$
2	6	1.8556	1.8556	1.8556	1.8556
3	10	3.4387	3.2403	3.2541	2.7936
4	15	4.4622	4.1734	4.1895	3.2358
5	21	5.9947	5.2375	5.2674	3.8526
6	28	8.0695	6.8737	6.9193	4.7738
7	36	9.8388	8.5045	8.5158	6.2232
8	45	12.0599	14.2730	10.9258	8.5089
9	55	15.0423	16.9076	13.6832	12.3057
10	66	19.2063	21.3786	17.7896	18.5947
11	78	25.3897	26.9520	23.3292	29.2915
12	91	34.1437	35.6501	31.4112	47.5801
13	105	47.1800	47.8854	42.8654	79.2277
14	120	65.8074	66.3107	59.6859	134.6209

4 Conclusions

We have developed several systematic techniques to partition a one and two-dimensional simplex by using the well-known Voronoi diagram and its variants. The resulted partitions have layered structure and the sub-cells concentrate near the edges. These two properties are found to be crucial for the partitions which lead to spectral volume reconstructions with small Lebesgue constants.

The spectral volume reconstructions on those partitions have small Lebesgue constants, one of which is roughly twice the Lebesgue constant of the same order interpolation based on the almost optimal nodal sets. The total number of edges (the total work when being used in spectral volume method) of the partitions is showed to be at most twice the minimum number of edges of all partitions for the reconstructions of the same order accuracy. When using the Dubiner basis, the spectral volume reconstruction matrix is very well-conditioned. All of these suggest that the partitions are a good choice for the spectral volume methods and other numerical methods which rely on reconstructions from cell averages.

Acknowledgment: The author thanks Prof. Franco P. Preparata for many helpful suggestions, and greatly appreciates the guidance and support of Prof. David Gottlieb and Prof. Jan S. Hesthaven. The author would also like to thank Prof. Z.J. Wang. We have this project from his seminar talk.

References

- [1] Q. Chen and I. Babuška. Approximate optimal points for polynomial interpolation of real functions in an interval and in a triangle. *Computer Methods in Applied Mechanics and Engineering*, 128:405–417, 1995.
- [2] P. J. Davis. *Interpolation and Approximation*. Dover Publications, New York, 1975.
- [3] M. de Berg, M. van Kreveld, M. Overmars, and O. Schwarzkopf. *Computational Geometry: algorithms and applications*. Springer-Verlag, 2nd edition, 2000.
- [4] M. Dubiner. Spectral methods on triangles and other domains. *Journal of Scientific Computing*, 6:345–390, 1993.
- [5] L. Fêjer. Bestimmung derjenigen abszissen eines intervalles, für welche die quadratsumme der grundfunktionen der lagrangeschen interpolation im intervall $[-1,+1]$ ein möglichst kleine maximum besitzt. *annali della Scuola Norm. Sup. di Pisa*, 1(2):3–16, 1932.
- [6] J. S. Hesthaven. From electrostatics to almost optimal nodal sets for polynomial interpolation in a simplex. *SIAM Journal on Numerical Analysis*, 35(2):655–676, 1998.
- [7] F. P. Preparata and M. I. Shamos. *Computational Geometry: An Introduction*. Springer-Verlag, New York, 1985.
- [8] M. A. Taylor, B. A. Wingate, and R. E. Vincent. An algorithm for computing fekete points in the triangle. *SIAM Journal On Numerical Analysis*, 38(5):1707–1720, 2000.
- [9] Z. Wang and Y. Liu. Spectral (finite) volume method for conservation laws on unstructured grids iii: One dimensional systems and partition optimization. *Journal of Scientific Computing*, 20(1):137–157, 2004.
- [10] Z. J. Wang. Spectral (finite) volume method for conservation laws on unstructured grids: Basic formulation. *Journal of Computational Physics*, 178:210–251, 2002.

- [11] Z. J. Wang and Y. Liu. Spectral(finite) volume method for conservation laws on unstructured grids. *Journal of Computational Physics*, 179:665–697, 2002.
- [12] M. Zhang and C.-W. Shu. An analysis of and a comparison between the discontinuous galerkin and the spectral finite volume methods. *Computers and Fluids*, 34:581–592, 2005.